DOI: 10.1002/ejoc.200600031

A New Method for the Formation of Anti-apicophilic (*O-cis*) Spirophosphoranes – Kinetic Studies on the Stereomutation of *O-cis* Arylspirophosphoranes to Their *O-trans* Isomers

Kazumasa Kajiyama,[a][‡] Miki Yoshimune,[a] Satoshi Kojima,[a] and Kin-ya Akiba*[‡‡]

Keywords: Anti-apicophilicity / Oxidation / Kinetics / Arylspirophosphorane / Pseudorotation

P–H spirophosphorane **4** bearing two Martin ligands was converted to dianions (**5a**–**n**), bearing R groups, with excess organolithium reagents (RLi). Subsequent oxidation with I_2 at ambient temperature gave *anti*-apicophilic (*O-cis*) spirophosphoranes **2a**–**n**. All *anti*-apicophilic phosphoranes **2a**–**n** isomerized irreversibly to the *O-trans* spirophosphoranes **3a**–**n**, respectively. For 2,6-dialkylphenyl derivatives **2k**–**n**, the barrier for pseudorotation between enantiomers **2**-R_P and **2**-S_P was rather high, and thus the interconversion could not be observed on the NMR timescale. The activation parameters for the pseudorotation of the triisopropylphenyl (TIP) derivative **2n** to **3n** were almost identical with those of *n*Bu derivative **2b** to **3b**, i.e., $\Delta H^{\ddagger}$ = 21.3 kcal mol^{-1}, $\Delta S^{\ddagger}$ = –9.4 eu.

Introduction

Interest in the chemistry of hypervalent[1] 10–P–5[2] phosphoranes stems from studies aimed at elucidating the reaction mechanism of processes such as phosphoryl transfer and hydrolysis of phosphates in biological systems. Most stable phosphoranes assume trigonal bipyramidal (TBP) structures in which there are two distinctive sites, the apical and the equatorial sites. The equatorial bonds can roughly be described as involving the sp^2 orbitals of the P atom, while the apical bonds can be explained with the concept of the three-center four-electron bond (3c–4e).[3] Since the electrons of the apical bonds can be delocalized into the apical substituents, electronegative substituents are preferred in these apical sites to relieve electron density upon the central atom. This gives rise to the concept of apicophilicity.[1,4] The site preference of the substituents is also dependent on steric bulk, that is, the bulky substituents are generally preferred in the less congested equatorial sites relative to the apical sites.

The fast stereomutation of the phosphoranes is reasonably explained by the Berry pseudorotation (BPR) process,[5] which is based on bond bending. In this mechanism, the two apical substituents exchange places with two equatorial substituents via a square pyramidal (SP) structure with the remaining equatorial substituent being the pivot. There are two fundamental methods for raising the stereomutation barrier between stable isomers interconverting via multiple numbers of BPR steps. One is to increase as much as possible the difference in apicophilicity between the apical and equatorial substituents. This should lead to increased relative stability of the more stable isomers. The other is the incorporation of small rings (five members or less) into the compound to introduce into the multi-step BPR process strained and thus highly unstable intermediates in which the small ring should span between two equatorial sites.

By incorporating the Martin ligand, which utilizes the Thorpe–Ingold effect,[6] we have recently succeeded in the first isolation and characterization of anti-apicophilic *O-cis* alkylphosphoranes **2a**–**c**, which are high energy configurational isomers of ordinary *O-trans* phosphoranes **3a**–**c**, in which the two oxygen atoms occupy the apical positions. The synthesis of **2a**–**c** was accomplished via thermal cyclization reactions of P–H (apical) monocyclic phosphoranes **1a**–**c** (Scheme 1) in pyridine.[7] In order to gain a compre-

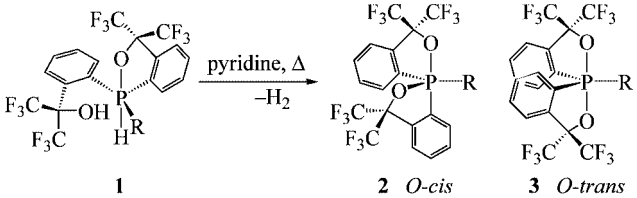

Scheme 1.

[a] Department of Chemistry, Graduate School of Science, Hiroshima University,
1-3-1 Kagamiyama, Higashi-Hiroshima 739-8526, Japan
[‡] Present address: Department of Chemistry, School of Science, Kitasato University,
1-15-1 Kitasato University, Sagamihara, Kanagawa 228-8555, Japan
[‡‡] Present address: Advanced Research Center for Science and Engineering, Waseda University,
3-4-1 Ohkubo, Shinjuku-ku, Tokyo 169-8555, Japan
E-mail: akibaky@waseda.jp

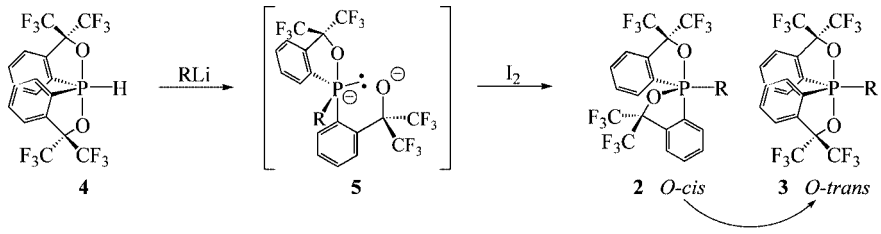

a) R = Me, **b)** R = *n*Bu, **c)** R = *t*Bu, **d)** R = Ph, **e)** 4-*tert*-butylphenyl, **f)** R = 4-methoxyphenyl, **g)** R = 4-(dimethylamino)phenyl, **h)** R = 2-methylphenyl, **i)** R = 4-methoxy-2,6-dimethylphenyl, **j)** R = 4-(dimethylamino)-2,6-dimethylphenyl, **k)** R = 2,6-dimethylphenyl, **l)** R = 2,4,6-trimethylphenyl, **m)** R = 2,4,6-triethylphenyl, **n)** R = 2,4,6-triisopropylphenyl

Scheme 2.

hensive understanding of this unique group of compounds en route to unveiling the whole multi-step BPR process, we decided to look into *O*-*cis* compounds with an aryl monodentate ligand. Because of the electronegative nature of aryl groups compared with alkyl groups, we envisioned that the preparation would be troublesome. Indeed, P–H (apical) compounds **1**, which are precursors to the *O*-*cis* compounds could not be obtained initially. In order to establish a milder method for the preparation of *O*-*cis* compounds, we briefly examined the use of oxidizing reagents. As a result, we found that the preparation of *O*-*cis* **2** could be achieved by I_2 oxidation of the dianion **5**, which is generated by the reaction of an excess of organolithium reagents with P–H phosphorane **4** (Scheme 2) without the need to isolate intermediate P–H (apical) phosphoranes **1a**–**c**.[7b,9] This has enabled us to isolate and characterize the first anti-apicophilic phosphorane with a monodentate aryl group. Herein we describe details of the generation of *O*-*cis* **2** by I_2 oxidation of **5**, and the effects of substituents on the monodentate aryl ring of *O*-*cis* arylphosphoranes on the stereomutation process, along with a kinetic study on the stereomutation of *O*-*cis* **2k**–**n** to *O*-*trans* **3k**–**n**.

Results and Discussion

The dianions **5**, formed in-situ by the treatment of P–H (equatorial) spirophosphorane **4** with excess organolithium reagents, were oxidized by I_2 in Et_2O to afford *O*-*cis* phosphoranes **2** at room temperature (Scheme 2).[8] Although the quantitative generation of the dianions **5a**–**c** could be achieved with ca. 3 equiv. of aliphatic lithium reagents, it was necessary to apply reagents in larger excesses in the case of aromatic lithium reagents (typically 6 equiv.) to afford the dianions **5d**–**n**. The ^{31}P NMR chemical shifts assignable to *O*-*cis* **2**, *O*-*trans* **3**, and dianions **5** in the reaction mixture are shown in Table 1. The phosphorus resonances of the dianions **5** appeared as broad singlets, and the chemical shifts of these species were similar to those observed for 10–P–4 species[10] despite the presence of bond switching equilibria of P–O bonds via either 8–P–3 or 12–P–5 species. As previously reported for alkyl-substituted **2a**–**c** and **3a**–**c**, ^{31}P NMR signals for **2d**–**n** were at lower field than those for **3d**–**n** in the aryl-substituted series. In the case of *O*-*cis* **2h**, two phosphorus resonances were observed, due to rotational isomers about the phosphorus–carbon bond of

Table 1. ^{31}P NMR chemical shifts of *O*-*cis* **2**, *O*-*trans* **3**, and dianion **5**, and the ratio of **2** and **3** after oxidation.

			^{31}P NMR chemical shift in Et_2O [δ]			Ratio of *O*-*cis* **2**/*O*-*trans* **3**	
Entry		R	**2**	**3**	**5**	directly after	after 30 min
1	**a**	methyl	–6.3	–22.6	–35.5	>99:<1	96:4
2	**b**	*n*-butyl	–3.5	–18.8	–23.1	>99:<1	>99:<1
3	**c**	*tert*-butyl	7.7	–9.8	–10.1	>99:<1	>99:<1
4	**d**	phenyl	–8.6	–31.9	[a]	27:73	<1:>99
5	**e**	4-*tert*-butylphenyl	–8.5	–32.5	[a]	71:29	<1:>99
6	**f**	4-methoxyphenyl	–8.3	–33.1	[a]	72:28	<1:>99
7	**g**	4-(dimethylamino)phenyl	–9.2	–33.8	[a]	87:13	25:75
8	**h**	2-methylphenyl	–5.6, –8.8	–26.6	–15.4	>99:<1	23:77
9	**i**	4-methoxy-2,6-dimethylphenyl	–3.6	–26.5	–13.0	>99:<1	53:47
10	**j**	4-(dimethylamino)-2,6-dimethylphenyl	–3.4	–25.6	–11.0	>99:<1	66:34
11	**k**	2,6-dimethylphenyl (DMP)	–4.7	–26.4	–9.2	>99:<1	54:66
12	**l**	2,4,6-trimethylphenyl (TMP)	–3.9	–26.2	–9.8	>99:<1	62:38
13	**m**	2,4,6-triethylphenyl (TEP)	–3.1	–25.8	–10.8	>99:<1	63:37
14	**n**	2,4,6-triisopropylphenyl (TIP)	–2.7	–25.7	–10.8	>99:<1	>99:<1

[a] The dianionic species could not be observed.

the 2-methylphenyl monodentate group (Table 1, run 8). The two alkyl groups in the 2- and 6-positions of the monodentate aryl group were also observed separately in **2i**–**n**, thus indicating that at least on the NMR timescale, the P–C bond rotation for the monodentate group is slow. The corresponding rotational barrier for **3h** was also high, as evident from the presence of four CF_3 signals in the ^{19}F NMR spectrum.

In the room-temperature ^{19}F NMR spectra of the *O-cis* alkyl derivatives **2a**–**c**, signals for the four anisochronous trifluoromethyl groups were observed as a pair of quartets due to fast interconversion between enantiomers **2-R_P** and **2-S_P** by a single step pseudorotation with the R group as the pivot (Figure 1).[5,7] However, for the *O-cis* 2,6-dialkylphenyl derivatives, ^{19}F NMR spectra of the crude products after workup at room temperature showed either three (**2i**–**l**) or four signals (**2m**, **n**), indicating the presence of a slower corresponding BPR process for the 2,6-dialkylphenyl derivatives. This should be a consequence of the steric hindrance exerted by the *ortho* alkyl groups as evident from the decelerated P–C bond rotation (vide supra).

The ratios of *O-cis* **2** and *O-trans* **3** in Et_2O at room temperature were determined by ^{31}P NMR spectroscopy immediately after the addition of I_2 and 30 min later (Table 1). Unlike the thermal method that required elevated temperatures, the exclusive generation of *O-cis* **2** could be observed for the alkyl derivatives **2a**–**c** right after oxidation (Table 1, entries 1–3). In the case of phenyl derivative **2d**, however, the *O-cis* isomer was the minor product, and pseudorotation to *O-trans* **3d** was complete within 30 min at room temperature (Table 1, entry 4), probably due to the higher apicophilicity of the phenyl group compared with alkyl groups in general.[11] In order to raise the BPR barrier by raising the energies of species such as B-R_P and B-S_P in a typical multi-step BPR process such as in Figure 2, compounds **2e**–**g**, bearing electron donating groups (*t*Bu, OMe, NMe_2, respectively) in the 4-positions of the monodentate aryl groups were examined. Although the *O-cis* isomer became the major product upon oxidation, this perturbation was not enough to allow isolation or detailed characterization. The incorporation of one methyl group at an *ortho* position of the monodentate aryl group (**2h**) was also not sufficient (Table 1, entry 8). However, the use of bulky aryl groups with two *ortho* substituents[12] led to the exclusive formation of the *O-cis* isomer, and these products (**2i**–**n**) were found to have sufficient lifetimes for characterization by ^1H NMR (Table 1, entries 9–14). Especially in the case of the TIP derivative, the *O-cis* isomer **2n** could be purified by silica gel chromatography (yield 71%) and further characterized by single crystal X-ray analysis (vide infra). The 1,3,5-tris(*t*Bu)phenyl group was found to be too bulky to be incorporated. The small $^1J_{P\text{-}C}$ value of 44.5 Hz for **2n** (com-

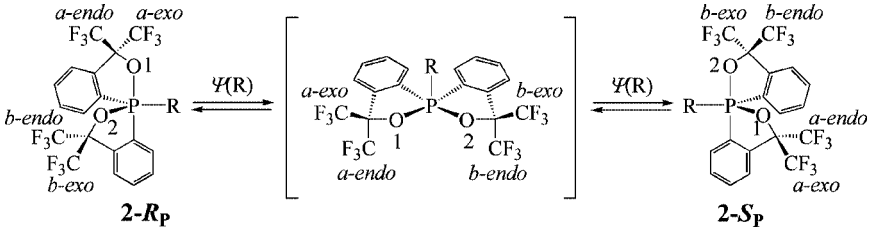

Figure 1. Interconversion between enantiomers **2-R_P** and **2-S_P** by a single step pseudorotation. The groups designated *exo* and *endo* cannot interconvert with this process.

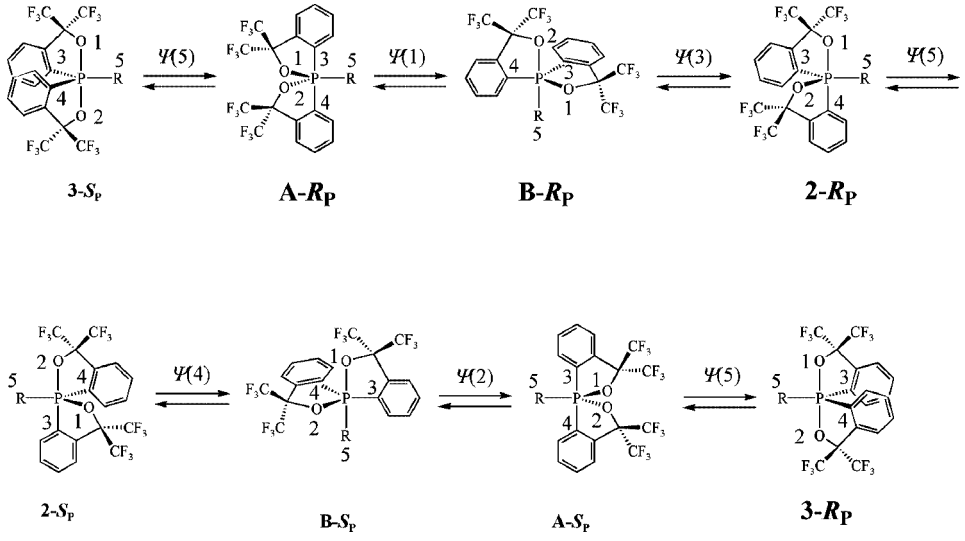

Figure 2. A multi-step pseudorotation process between the most stable isomers, *O-trans* **3-S_P** and **3-R_P**.

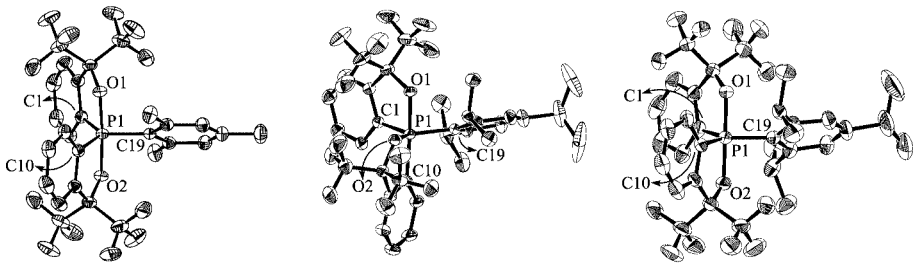

Figure 3. The ORTEP drawings of **3l** (left), **2n** (middle), and **3n** (right) showing the thermal ellipsoids at the 30% probability level. All the hydrogens have been omitted for clarity.

pared with 125.2 and 115.9 for the other two $^1J_{P\text{-}C}$ values of equatorial carbons) clearly indicates the presence of coupling between P and an apical carbon.

The X-ray structures of *O-cis* **2n** and *O-trans* **3l** and **3n** are depicted in Figure 3, with selected structural parameters listed in Table 2. *O-trans* **3l** and **3n** assumed slightly distorted TBP structures and were quite symmetric, with the apical P–O and equatorial P–C bond lengths of the Martin ligands being practically the same. While the sum of the three equatorial bond angles of 358.1° for *O-cis* **2n** was nearly identical to the ideal value of 360°, the apical bond (168.9°) was more distorted than that of *O-trans* **3n** (178.8°). In the crystal structure of *O-cis* **2n**, the apical bonds of the bidentate groups were significantly longer than the corresponding equatorial bonds [P1–O1(apical): 1.777 > P1–O2(equatorial): 1.678 Å and P1–C10(apical): 1.885 > P1–C1(equatorial): 1.818 Å] as anticipated from the difference in the bonding scheme between the apical and equatorial bonds and coinciding nicely with $^1J_{P\text{–}C}$ values (vide supra).

Table 2. Selected bond lengths and angles for **2n**, **3n**, and **3l**.

	3l	**2n**	**3n**
	Bond lengths [Å]		
P1–O1	1.754(1)	1.777(1)	1.757(3)
P1–O2	1.754(1)	1.678(1)	1.763(3)
P1–C1	1.826(2)	1.818(2)	1.820(3)
P1–C10	1.826(2)	1.885(2)	1.825(4)
P1–C19	1.837(2)	1.865(2)	1.845(4)
	Bond angles [°]		
O1–P1–O2	175.5(1)	82.4(1)	178.8(2)
O1–P1–C1	87.0(1)	86.8(1)	87.1(2)
O1–P1–C10	90.8(1)	168.9(1)	92.8(2)
O1–P1–C19	92.3(4)	86.9(1)	91.6(2)
O2–P1–C1	90.8(1)	114.0(1)	91.8(2)
O2–P1–C10	87.0(1)	86.5(1)	87.4(2)
O2–P1–C19	92.3(4)	123.0(1)	89.3(2)
C1–P1–C10	122.9(1)	98.3(1)	115.8(2)
C1–P1–C19	118.6(4)	121.1(1)	123.6(2)
C10–P1–C19	118.6(4)	98.8(1)	120.6(2)

Holmes has proposed a method of determining the degree of structural distortion of pentacoordinate compounds from TBP towards the transition state structure of square pyramidal structure (SP) on the BPR coordinate, based upon calculations involving internal angles of the pentacoordinate species.[13] Using this method, Holmes has demonstrated that the structural distortions of nonmetalated spirophosphoranes follow a BPR process from TBP towards SP geometry in which the monodentate substituent occupies the axial site and the bidentate substituents occupy the four basal sites. The percent distortions estimated by the dihedral angle method using unit bond lengths[13,14] for compounds structurally determined in this study are given in Table 3. If a distortion is along a certain Berry coordinate, the sum of percent distortion from TBP to RP(SP) (RP = rectangular pyramid) and that from RP(SP) to TBP should be nearly 100%, as seen for *O-trans* **3b** (R = *n*Bu) and **3l** (R = 2,4,6-trimethylphenyl) with C19 as the pivot. An analysis revealed that the TBP geometry of *O-cis* **2c** (R = *t*Bu) was distorted toward the transition state of the interconversion between **2c**-$\boldsymbol{R_P}$ and **2c**-$\boldsymbol{S_P}$ with the monodentate group as the pivot, whereas the distortion of *O-cis* **2b** (R = *n*Bu) was along the BPR coordinate towards B with C10, a carbon of a bidentate group, as the pivot. This is consistent with the barrier for the interconversion of enantiomers of **2b** being higher than that for enantiomers of **2c**.[7b] As for **2n** and **3n**, the sums of percent distortion from TBP to SP and that from SP to TBP are 102%, but only one equatorial angle (O2–P1–C1 for **2n**: 114.0° and C1–P1–C10 for **3n**: 115.8°) is smaller than the ideal value of 120°. Similar distortion has been found in a few phosphoranido complexes.[15] Additionally, the equatorial P–O bond of **2n** (1.678 Å) was somewhat longer than those of alkyl derivatives **2b** (1.658 Å) and **2c** (1.652 Å), despite the apical P–O bond length of **2n** (1.777 Å) being comparable to those of the alkyl derivatives **2b** (1.773 Å) and **2c** (1.771 Å).[7] Thus, the distortion from TBP geometry of **2n** and **3n** does not follow any pseudorotation process. This is

Table 3. Percent distortion (%) of phosphorane structures.

	pivot: C19 TBP to RP	RP to TBP	pivot: C1 TBP to SP	SP to TBP
2b	20	96	20	85
3b	17	83	17	108
2c	13	88	13	104
3l	10	90	10	105
2n	15	103	15	87
3n	8	106	8[a]	94[a]

[a] Pivot: C10.

clearly due to the bulkiness of the TIP group which makes the approach of the other two equatorial ligands, which is required for pseudorotation to proceed, difficult. Thus, the structural distortion is in good agreement with the high barrier for the pseudorotation between enantiomers of **2n** compared with **2b** or **2c**. The pseudorotation of the TIP-substituted bis(4,4′-dimethyl-2,2′-biphenylyl)phosphorane has also been reported not to follow the simplest Berry pseudorotation process with the TIP group as the pivot.[12]

The stereomutation rates of *O-cis* **2k**–**n** to *O-trans* **3k**–**n** were measured in toluene (273–293 K for **2k**–**m** to **3k**–**m**, 313–333 K for **2n** to **3n**) by monitoring the ^{19}F NMR signals of the change in ratio of **2** and **3**. All of the measured processes followed first-order kinetics. In the case of the pseudorotation of *O-cis* TIP phosphorane **2n** to *O-trans* **3n**, the rates in acetic acid were also measured. The Eyring plot of the rates turned out to be linear (Figure 4, Figure 5), which implies that there are no competing pathways for the stereomutation. Representative rates and activation parameters are shown in Table 4. The stereomutation of **2n** was found to be much slower than that for **2k**–**m** with the difference in $\Delta G^{\ddagger}$ between **2n** ($\Delta G^{\ddagger}$ = 24.1 kcal mol^{-1}) and **2l** ($\Delta G^{\ddagger}$ = 22.2 kcal mol^{-1}) being 1.9 kcal mol^{-1} at 293 K. On the other hand, the difference in stereomutation rate among **2k**–**m** in toluene was very small but observable, and in agreement with expectations. The rate was smallest for the most sterically hindered triethylphenyl-substituted **2m**, and coming in second was **2l**, which has three (one more than **2k**) electron-donating methyl groups on the monodentate aryl group. Incidentally, the activation parameters for the stereomutation in toluene of the TIP derivative **2n** ($\Delta H^{\ddagger}$ = 21.3 kcal mol^{-1} and $\Delta S^{\ddagger}$ = –9.4 eu) were essentially the same as those for the *n*Bu derivative **2b** ($\Delta H^{\ddagger}$ = 21.8 kcal mol^{-1} and $\Delta S^{\ddagger}$ = –9.0 eu),[7] indicating that significant modification is required to make the apicophilicity of aryl groups comparable with alkyl groups. The use of AcOH as solvent did not lead to a significant increase in rate. Therefore it is safe to believe that the stereomutation process is of BPR in nature, without contribution from pathways involving bond-dissociation and recombination as rate-determining steps. This is in agreement with previously reported stereomutation between diastereomeric *O-trans* stiboranes.[16] It must be pointed out that there is a possibility that the turnstile mechanism is the actual pathway.[17] Unfortunately, we presently have no experimental means to judge the validity of this often-proposed mechanism.

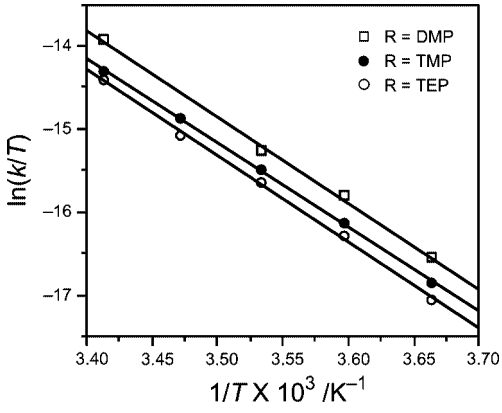

Figure 4. Eyring plots for the stereomutation of *O-cis* **2k**–**m** to *O-trans* **3k**–**m** in toluene at 273–293 K.

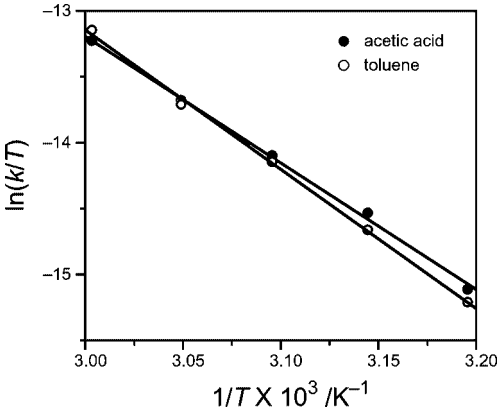

Figure 5. Eyring plot for the stereomutation of *O-cis* **2n** to *O-trans* **3n** in toluene and in acetic acid at 313–333 K.

In conclusion, the generation of anti-apicophilic *O-cis* arylspirophosphoranes **2d**–**n** at room temperature could be achieved by the I_2 oxidation of the dianions **5** formed by the treatment of P–H (equatorial) spirophosphorane **4** with excess aryllithium reagents. On the basis of the *O-cis* **2**/*O-trans* **3** ratios in the reaction mixtures determined by ^{31}P NMR analyses, the stabilities of the *O-cis* arylphosphoranes towards stereomutation to *O-trans* arylphosphoranes seemed to be more dependent on steric bulk than the electronic character of the monodentate aryl substituents. The ^{19}F NMR spectra showed the isomerization between enantiomers of *O-cis* arylphosphoranes to be slower than that of *O-cis* alkylphosphoranes. Only *O-cis* TIP phosphorane **2n** could be isolated in the *cis* series. The crystal structures of *O-cis* **2n** and *O-trans* **3l** and **3n** could be determined by X-ray structural analyses, and the TIP derivatives **2n** and **3n** were verified to be geometrical isomers. The per-

Table 4. Representative rates and activation parameters for the permutation of *O-cis* **2k**–**n** to *O-trans* **3k**–**n**.[a]

Entry	R		Solvent	k [s^{-1}] (T [K])	$\Delta G^{\ddagger}$ [kcal mol^{-1}] (T [K])	$\Delta H^{\ddagger}$ [kcal mol^{-1}]	$\Delta S^{\ddagger}$ [eu]
1	DMP	**k**	toluene	$(2.61 \pm 0.05) \times 10^{-4}$ (293)	21.9 (293)	20.4 ± 1.0	–5.4 ± 3.6
2	TMP	**l**	toluene	$(1.81 \pm 0.01) \times 10^{-4}$ (293)	22.2 (293)	20.0 ± 0.5	–7.5 ± 1.8
3	TEP	**m**	toluene	$(1.60 \pm 0.02) \times 10^{-4}$ (293)	22.2 (293)	20.4 ± 0.7	–6.4 ± 2.4
4	TIP	**n**	toluene	$(6.26 \pm 0.07) \times 10^{-4}$ (333)	24.4 (333)	21.3 ± 0.7	–9.4 ± 2.0
5	TIP	**n**	acetic acid	$(5.98 \pm 0.13) \times 10^{-4}$ (333)	24.5 (333)	19.5 ± 0.8	–15.0 ± 2.5

[a] Error is given as standard deviation.

cent distortion along the Berry pseudorotation coordinate estimated by the dihedral angle method suggested that the TBP structures of **2b** and **2c** were distorted towards SP geometry, leading to the enantiomer of **2b** and an intermediate en route to *O*-*trans* **3c**, respectively. As for the TIP derivatives **2n** and **3n**, the distortion from TBP geometry did not follow any pseudorotation process due to the extremely large steric repulsion between the TIP group and the other equatorial ligands. Kinetic measurements of the *O*-*cis* to *O*-*trans* pseudorotation process demonstrated that the activation parameters for TIP derivative **2n** were identical with those for *n*Bu derivative **2b**.

Experimental Section

Melting points were measured with a Yanaco micro melting point apparatus and are uncorrected. ^{1}H NMR (400 MHz), ^{13}C NMR (100 MHz), ^{19}F NMR (376 MHz), and ^{31}P NMR (162 MHz) spectra were recorded on a JEOL EX-400 spectrometer. ^{1}H NMR chemical shifts (δ) are given in ppm downfield from internal Me_4Si or from residual chloroform-*d* (δ = 7.26). ^{13}C NMR chemical shifts (δ) are given in ppm from chloroform-*d* (δ = 77.0). ^{19}F NMR chemical shifts (δ) are given in ppm downfield from external $CFCl_3$. ^{31}P NMR chemical shifts (δ) are given in ppm downfield from external 85% H_3PO_4. Elemental analyses were performed on a Perkin–Elmer 2400 CHN elemental analyzer. All reactions were carried out under N_2. Et_2O was freshly distilled from Na-benzophenone. Acetic acid was distilled from P_2O_5. Toluene was distilled from CaH_2. 4-Bromo-3,5-dimethylanisole,[18] bromo-2,4,6-triethylbenzene,[12] bromo-2,4,6-triisopropylbenzene,[12] and phosphorane **4**[19] were prepared according to published procedures. Preparative thin layer chromatography was carried out on plates of Merck silica gel 60 GF254.

[*TBPY*-5-12]- and [*TBPY*-5-11]-1-Methyl-3,3,3′,3′-tetrakis(trifluoromethyl)-1,1′-spirobi[3*H*,2,1,λ^5-benzoxaphosphole] (2a and 3a): To a solution of **4** (3.01 g, 5.83 mmol) in Et_2O (50 mL) was added MeLi (17.0 mL, 17.3 mmol, 1.02 M in Et_2O) at 0 °C, and the mixture was stirred for 3 h at room temperature. I_2 (4.50 g, 17.7 mmol) was then added to the solution at –78 °C, and the mixture was stirred for 1 h. The resulting mixture was washed with aq. $Na_2S_2O_3$ (120 mL) and brine (100 mL), dried with anhydrous $MgSO_4$, and the solvent was evaporated in vacuo with cooling (acetone/CO_2 bath). The resulting crude solid was washed with *n*-hexane to afford white solid **2a**[7b] (2.64 g, 83%) containing a small portion (8%) of **3a**.[7b]

[*TBPY*-5-12]-1-Butyl-3,3,3′,3′-tetrakis(trifluoromethyl)-1,1′-spirobi[3*H*,2,1,λ^5-benzoxaphosphole] (2b): To a solution of **4** (3.09 g, 5.99 mmol) in Et_2O (50 mL) was added *n*BuLi (11.7 mL, 18.0 mmol, 1.52 M in hexane) at 0 °C, and then the solution was stirred for 3 h at room temperature. The solution was cooled to –78 °C, and then I_2 (4.60 g, 18.1 mmol) was added. The mixture was stirred for 1 h at –78 °C, and the resulting solution was washed with aq. $Na_2S_2O_3$ (2× 50 mL) and brine (2× 50 mL). The organic layer was dried with anhydrous $MgSO_4$ and concentrated in vacuo. The resulting crude product was washed with *n*-hexane to afford **2b**[7b] as a white solid (3.12 g, 91%).

[*TBPY*-5-12]-1-(1,1-Dimethyl)ethyl-3,3,3′,3′-tetrakis(trifluoromethyl)-1,1′-spirobi[3*H*,2,1,λ^5-benzoxaphosphole] (2c): To a solution of **4** (1.01 g, 1.95 mmol) in Et_2O (20 mL) was added *t*BuLi (4.00 mL, 6.48 mmol, 1.6 M in pentane) at 0 °C, and the solution was stirred for 3 h at room temperature. The solution was cooled to –78 °C, and then I_2 (1.65 g, 6.50 mmol) was added. The mixture was stirred for 1 h at –78 °C. The resulting solution was washed with aq. $Na_2S_2O_3$ (2× 30 mL) and brine, the organic layer was dried with anhydrous $MgSO_4$, and the solvents were evaporated. The resulting crude solid was recrystallized from acetonitrile to afford **2c**[7b] as colorless crystals (529 mg, 48%).

4-Bromo-*N*,*N*,3,5-tetramethylaniline:[17] Benzyltrimethylammonium tribromide[20] was added to a solution of *N*,*N*-3,5-tetramethylaniline (2.00 mL, 12.2 mmol) in CH_2Cl_2 (50 mL) and MeOH (20 mL) at room temperature to give an orange-colored solution. The solution was stirred for 5 min until it became discolored. The solvent was evaporated in vacuo and 10% KOH aq. was added to neutralize. The mixture was extracted with Et_2O (3× 50 mL), the combined organic layer was dried with anhydrous K_2CO_3, and then the solvent was removed. The crude product was distilled to afford a colorless liquid (2.19 g, 79%). Bp 86 °C (0.15 Torr). ^{1}H NMR ($CDCl_3$): δ = 6.52 (s, 2 H), 2.95 (s, 6 H), 2.43 (s, 6 H) ppm.

General Procedure for the Synthesis of Arylphosphoranes: To a solution of ArBr (2.72 mmol) in Et_2O (5 mL) was added *n*BuLi (1.46 mL, 2.33 mmol, 1.62 M in hexane) at –78 °C. Except for the lithiation of anisole derivatives, the mixture was warmed to room temperature and stirring was continued for 3 h or 12 h (for aniline derivatives). 4-Bromoanisole and 4-bromo-3,5-dimethylanisole were lithiated at 0 °C for 8 h. To the solution of ArLi was added a solution of **4** (0.388 mmol) in Et_2O (5 mL) at –78 °C, and stirring was continued at room temperature for 1 h, followed by the addition of I_2 (2.33 mmol). Within five min, the resulting solution was washed with aq. $Na_2S_2O_3$, and the mixture was extracted with Et_2O (20 mL × 3). The collected organic layer was dried with anhydrous $MgSO_4$, and the solvent was evaporated in vacuo. The crude product was purified by PTLC (silica gel, hexane:CH_2Cl_2 = 3:1), followed by recrystallization from hexane/CH_2Cl_2 to give **3** (or **2n**) as colorless crystals.

[*TBPY*-5-11]-1-(2-Methyl)phenyl-3,3,3′,3′-tetrakis(trifluoromethyl)-1,1′-spirobi[3*H*,2,1,λ^5-benzoxaphosphole] (3h): 57%; m.p. 155 °C (sublimation). ^{1}H NMR ($CDCl_3$): δ = 8.64–8.58 (m, 2 H), 7.80–7.74 (m, 6 H), 7.40 (dd, $^3J_{HP}$ = 18.1 Hz, $^3J_{HH}$ = 7.8 Hz, 1 H), 7.40 (t, $^3J_{HH}$ = 7.8 Hz, 1 H), 7.05–7.02 (m, 2 H), 2.29 (s, 3 H) ppm. ^{19}F NMR ($CDCl_3$): δ = –74.9 (q, $^4J_{FF}$ = 9.7 Hz, 3F), –75.0 (q, $^4J_{FF}$ = 9.7 Hz, 3F), –75.7 (q, $^4J_{FF}$ = 9.7 Hz, 3F), –75.8 (q, $^4J_{FF}$ = 9.7 Hz, 3F) ppm. ^{31}P NMR ($CDCl_3$): δ = –27.5 ppm. $C_{25}H_{15}F_{12}O_2P$: calcd. C 49.52, H 2.49; found C 49.34, H 2.31.

[*TBPY*-5-11]-1-(2,6-Dimethyl-4-methoxy)phenyl-3,3,3′,3′-tetrakis(trifluoromethyl)-1,1′-spirobi[3*H*,2,1,λ^5-benzoxaphosphole] (3i): 27%; m.p. 172 °C (sublimation). ^{1}H NMR ($CDCl_3$): δ = 8.48–8.44 (m, 2 H), 7.72–7.68 (m, 6 H), 6.40 (d, $^4J_{HP}$ = 5.4 Hz, 2 H), 3.74 (s, 3 H), 2.22 (s, 6 H) ppm. ^{19}F NMR ($CDCl_3$): δ = –74.2 (q, $^4J_{FF}$ = 9.8 Hz, 6F), –75.7 (q, $^4J_{FF}$ = 9.8 Hz, 6F) ppm. ^{31}P NMR ($CDCl_3$): δ = –27.3 ppm. $C_{27}H_{19}F_{12}O_3P$: calcd. C 49.86, H 2.94; found C 49.91, H 2.56.

[*TBPY*-5-11]-1-(4-Dimethylamino-2,6-dimethyl)phenyl-3,3,3′,3′-tetrakis(trifluoromethyl)-1,1′-spirobi[3*H*,2,1,λ^5-benzoxaphosphole] (3j): 9%; m.p. 147 °C (sublimation). ^{1}H NMR ($CDCl_3$): δ = 8.48–8.46 (m, 2 H), 7.71–7.66 (m, 6 H), 6.17 (s, 2 H), 2.89 (s, 6 H), 2.22 (s, 6 H) ppm. ^{19}F NMR ($CDCl_3$): δ = –67.8 (q, $^4J_{FF}$ = 9.8 Hz, 6F), –69.3 (q, $^4J_{FF}$ = 9.8 Hz, 6F) ppm. ^{31}P NMR ($CDCl_3$): δ = –26.6 ppm. $C_{28}H_{22}F_{12}NO_2P$: calcd. C 50.69, H 3.34, N 2.11; found C 50.40, H 3.08, N 1.84.

[*TBPY*-5-12]-1-(2,6-Dimethyl)phenyl-3,3,3′,3′-tetrakis(trifluoromethyl)-1,1′-spirobi[3*H*,2,1,λ^5-benzoxaphosphole] (2k): ^{1}H NMR ($CDCl_3$): δ = 7.82 (d, $^3J_{HH}$ = 7.3 Hz, 1 H), 7.65–7.62 (m, 3 H),

7.53–7.50 (m, 4 H), 7.18 (dd, $^4J_{HP}$ = 12.2 Hz, $^3J_{HH}$ = 7.3 Hz, 1 H), 7.10 (dt, $^5J_{HP}$ = 2.0 Hz, $^3J_{HH}$ = 7.3 Hz, 1 H), 6.95 (dd, $^4J_{HP}$ = 8.3 Hz, $^3J_{HH}$ = 7.3 Hz, 1 H), 2.72 (s, 3 H), 2.17 (s, 3 H) ppm. ^{19}F NMR ($CDCl_3$): δ = –72.9 (q, $^4J_{FF}$ = 9.8 Hz, 3F), –75.0 (br. s, 6F), –75.9 (q, $^4J_{FF}$ = 9.7 Hz, 3F) ppm. ^{31}P NMR ($CDCl_3$): δ = –5.7.

[*TBPY*-5-11]-1-(2,6-Dimethyl)phenyl-3,3,3′,3′-tetrakis(trifluoromethyl)-1,1′-spirobi[3*H*,2,1,λ^5-benzoxaphosphole] (3k): 68%; m.p. 122 °C (sublimation). ^{1}H NMR ($CDCl_3$): δ = 8.49–8.46 (m, 2 H), 7.74–7.70 (m, 6 H), 7.05 (dt, $^5J_{HP}$ = 2.4 Hz, $^3J_{HH}$ = 7.3 Hz, 1 H), 6.86 (dd, $^4J_{HP}$ = 6.8 Hz, $^3J_{HH}$ = 7.3 Hz, 2 H), 2.21 (s, 6 H) ppm. ^{19}F NMR ($CDCl_3$): δ = –74.1 (q, $^4J_{FF}$ = 9.8 Hz, 6F), –75.8 (q, $^4J_{FF}$ = 9.8 Hz, 6F) ppm. ^{31}P NMR ($CDCl_3$): δ = –27.3 ppm. $C_{26}H_{17}F_{12}O_2P$: calcd. C 50.34, H 2.76; found C 50.29, H 2.52.

[*TBPY*-5-12]-1-(2,4,6-Trimethyl)phenyl-3,3,3′,3′-tetrakis(trifluoromethyl)-1,1′-spirobi[3*H*,2,1,λ^5-benzoxaphosphole] (2l): ^{1}H NMR ($CDCl_3$): δ = 7.81 (d, $^3J_{HH}$ = 7.3 Hz, 1 H), 7.64–7.60 (m, 3 H), 7.56–7.42 (m, 4 H), 6.84 (d, $^4J_{HP}$ = 5.8 Hz, 1 H), 6.76 (d, $^4J_{HP}$ = 7.8 Hz, 1 H), 2.67 (s, 3 H), 2.22 (s, 3 H), 2.13 (s, 3 H) ppm. ^{19}F NMR ($CDCl_3$): δ = –74.5 (q, $^4J_{FF}$ = 9.7 Hz, 3F), –75.1 (br. s, 6F), –76.1 (q, $^4J_{FF}$ = 9.7 Hz, 3F) ppm. ^{31}P NMR ($CDCl_3$): δ = –5.2.

[*TBPY*-5-11]-1-(2,4,6-Trimethyl)phenyl-3,3,3′,3′-tetrakis(trifluoromethyl)-1,1′-spirobi[3*H*,2,1,λ^5-benzoxaphosphole] (3l): 64%; m.p. 175 °C (sublimation). ^{1}H NMR ($CDCl_3$): δ = 8.49–8.45 (m, 2 H), 7.72–7.66 (m, 6 H), 6.67 (d, $^4J_{HP}$ = 6.4 Hz, 2 H), 2.19 (s, 3 H), 2.18 (s, 6 H) ppm. ^{19}F NMR ($CDCl_3$): δ = –74.2 (q, $^4J_{FF}$ = 9.8 Hz, 6F), –75.7 (q, $^4J_{FF}$ = 9.8 Hz, 6F) ppm. ^{31}P NMR ($CDCl_3$): δ = –27.0 ppm. $C_{27}H_{19}F_{12}O_2P$: calcd. C 51.12, H 3.02; found C 51.02, H 2.90.

[*TBPY*-5-12]-1-(2,4,6-Triethyl)phenyl-3,3,3′,3′-tetrakis(trifluoromethyl)-1,1′-spirobi[3*H*,2,1,λ^5-benzoxaphosphole] (2m): ^{1}H NMR ($CDCl_3$): δ = 7.96–7.90 (m, 1 H), 7.88–7.84 (m, 3 H), 7.58–7.52 (m, 4 H), 7.39 (d, $^4J_{HP}$ = 6.4 Hz, 1 H), 7.36 (d, $^4J_{HP}$ = 6.4 Hz, 1 H), 2.96–2.64 (m, 6 H), 1.42 (t, $^3J_{HH}$ = 7.3 Hz, 3 H), 1.32 (t, $^3J_{HH}$ = 7.3 Hz, 3 H), 1.29 (t, $^3J_{HH}$ = 7.3 Hz, 3 H) ppm. ^{19}F NMR ($CDCl_3$): δ = –73.7 (q, $^4J_{FF}$ = 9.8 Hz, 3F), –74.6 (q, $^4J_{FF}$ = 9.8 Hz, 3F), –75.1 (q, $^4J_{FF}$ = 9.8 Hz, 3F), –75.2 (q, $^4J_{FF}$ = 9.8 Hz, 3F) ppm. ^{31}P NMR ($CDCl_3$): δ = –3.7 ppm.

[*TBPY*-5-11]-1-(2,4,6-Triethyl)phenyl-3,3,3′,3′-tetrakis(trifluoromethyl)-1,1′-spirobi[3*H*,2,1,λ^5-benzoxaphosphole] (3m): 16%. M.p. 157 °C (sublimation). ^{1}H NMR ($CDCl_3$): δ = 8.52–8.44 (m, 2 H), 7.76–7.64 (m, 6 H), 6.76 (d, $^4J_{HP}$ = 6.4 Hz, 2 H), 2.79 (dq, $^2J_{HH}$ = 14.6 Hz, $^3J_{HH}$ = 7.3 Hz, 2 H), 2.74 (dq, $^2J_{HH}$ = 14.6 Hz, $^3J_{HH}$ = 7.3 Hz, 2 H), 2.54 (q, $^3J_{HH}$ = 7.3 Hz, 2 H), 1.17 (t, $^3J_{HH}$ = 7.3 Hz, 3 H), 0.71 (t, $^3J_{HH}$ = 7.3 Hz, 6 H) ppm. ^{19}F NMR ($CDCl_3$): δ = –74.1 (q, $^4J_{FF}$ = 9.8 Hz, 6F), –75.1 (q, $^4J_{FF}$ = 9.8 Hz, 6F) ppm. ^{31}P NMR ($CDCl_3$): δ –26.6 ppm. $C_{30}H_{25}F_{12}O_2P$: calcd. C 53.27, H 3.72; found C 53.29, H 3.53.

[*TBPY*-5-12]-1-(2,4,6-Triisopropyl)phenyl-3,3,3′,3′-tetrakis(trifluoromethyl)-1,1′-spirobi[3*H*,2,1,λ^5-benzoxaphosphole] (2n): 71%. Mp 157 °C (decomp.). ^{1}H NMR ($CDCl_3$): δ = 7.80–7.75 (m, 2 H), 7.66–7.63 (m, 2 H), 7.57–7.52 (m, 2 H), 7.47–7.42 (m, 1 H), 7.20 (dd, $^3J_{HP}$ = 11.7 Hz, $^3J_{HH}$ = 7.8 Hz, 1 H), 7.08 (dd, $^4J_{HP}$ = 4.4 Hz, $^4J_{HH}$ = 1.9 Hz, 1 H), 6.95 (dd, $^4J_{HP}$ = 8.8 Hz, $^4J_{HH}$ = 1.9 Hz, 1 H), 3.94 (sept, $^3J_{HH}$ = 6.8 Hz, 1 H), 3.39 (sept, $^3J_{HH}$ = 6.8 Hz, 1 H), 2.83 (sept, $^3J_{HH}$ = 6.8 Hz, 1 H), 1.41 (d, $^3J_{HH}$ = 6.8 Hz, 3 H), 1.36 (d, $^3J_{HH}$ = 6.8 Hz, 3 H), 1.21 (d, $^3J_{HH}$ = 6.8 Hz, 6 H), 1.04 (d, $^3J_{HH}$ = 6.8 Hz, 3 H), 0.39 (d, $^3J_{HH}$ = 6.8 Hz, 3 H) ppm. ^{13}C NMR ($CDCl_3$): δ = 149.1 (d, J_{CP} = 9.3 Hz), 149.1, 142.7 (d, $^1J_{CP}$ = 44.5 Hz), 142.3 (d, J_{CP} = 21.7 Hz), 137.5 (d, $^1J_{CP}$ = 115.9 Hz), 136.9 (d, J_{CP} = 19.7 Hz), 134.2 (d, $^1J_{CP}$ = 125.2 Hz), 133.4 (d, J_{CP} = 2.1 Hz), 133.2 (d, J_{CP} = 16.6 Hz), 130.9 (d, J_{CP} = 15.5 Hz), 130.7 (d, J_{CP} = 19.7 Hz), 130.6, 130.4 (d, J_{CP} = 7.2 Hz), 130.3 (d, J_{CP} = 9.3 Hz), 125.5 (d, J_{CP} = 12.4 Hz), 125.0 (d, J_{CP} = 7.4 Hz), 123.6 (d, J_{CP} = 14.0 Hz), 122.7 (q, J_{CF} = 287.6 Hz), 122.3 (q, J_{CF} = 287.6 Hz), 122.2 (d, J_{CP} = 17.6 Hz), 121.8 (q, J_{CF} = 287.6 Hz), 121.7 (q, J_{CF} = 287.6 Hz), 81.4 (sept, J_{CF} = 31.3 Hz), 79.7 (sept, J_{CF} = 31.3 Hz), 33.7 (d, J_{CP} = 1.6 Hz), 32.9 (d, J_{CP} = 5.7 Hz), 31.7 (d, J_{CP} = 5.2 Hz), 25.4, 24.6, 24.4 (d, J_{CP} = 1.6 Hz) ppm. ^{19}F NMR ($CDCl_3$): δ = –74.1 (q, $^4J_{FF}$ = 9.8 Hz, 3F), –74.2 (q, $^4J_{FF}$ = 9.8 Hz, 3F), –74.3 (q, $^4J_{FF}$ = 9.8 Hz, 3F), –74.6 (q, $^4J_{FF}$ = 9.8 Hz, 3F) ppm. ^{31}P NMR ($CDCl_3$): δ = –2.8 ppm. $C_{33}H_{31}F_{12}O_2P$: calcd. C 55.16, H 4.35; found C 55.16, H 4.09.

[*TBPY*-5-11]-1-(2,4,6-Triisopropyl)phenyl-3,3,3′,3′-tetrakis(trifluoromethyl)-1,1′-spirobi[3*H*,2,1,λ^5-benzoxaphosphole] (3n): A solution of **2n** (50 mg, 0.07 mmol) in Et_2O (3 mL) was heated at 60 °C for 12 hours. The solvent was removed in vacuo and the residue was recrystallized from hexane/CH_2Cl_2 to afford **3n** quantitatively (50 mg, 0.07 mmol, 99%). Mp 144 °C. ^{1}H NMR ($CDCl_3$): δ = 8.45–8.40 (m, 2 H), 7.71–7.65 (m, 6 H), 6.88 (d, $^4J_{HP}$ = 6.4 Hz, 2 H), 3.74 (sept, $^3J_{HH}$ = 6.8 Hz, 2 H), 2.79 (sept, $^3J_{HH}$ = 6.8 Hz, 1 H), 1.21 (d, $^3J_{HH}$ = 6.8 Hz, 6 H), 1.17 (d, $^3J_{HH}$ = 6.8 Hz, 6 H), 0.46 (d, $^3J_{HH}$ = 6.8 Hz, 3 H) ppm. ^{13}C NMR ($CDCl_3$): δ = 149.5 (d, J_{CP} = 3.7 Hz), 148.7 (d, J_{CP} = 14.7 Hz), 136.8 (d, J_{CP} = 20.2 Hz), 136.4 (d, J_{CP} = 11.0 Hz), 135.0 (d, $^1J_{CP}$ = 178.3 Hz), 133.2 (d, J_{CP} = 3.7 Hz), 133.1 (d, $^1J_{CP}$ = 154.4 Hz), 131.2 (d, J_{CP} = 14.7 Hz), 124.8 (d, J_{CP} = 14.7 Hz), 122.7(d, J_{CP} = 16.5 Hz), 122.7 (q, J_{CF} = 288.6 Hz), 122.3 (q, J_{CF} = 288.6 Hz), 82.1 (sept, J_{CF} = 31.2 Hz), 33.7, 31.3 (d, J_{CP} = 5.5 Hz), 23.8, 23.6 ppm. ^{19}F NMR ($CDCl_3$): δ = –74.0 (q, $^4J_{FF}$ = 9.8 Hz, 6F), –74.8 (q, $^4J_{FF}$ = 9.8 Hz, 6F) ppm. ^{31}P NMR ($CDCl_3$): δ = –2.8 ppm. $C_{33}H_{31}F_{12}O_2P$: calcd. C 55.16, H 4.35; found C 54.99, H 4.19.

X-ray Crystal Structure Determination of 3l, 2n, and 3n: Crystals suitable for X-ray structure determination were mounted on a Mac Science MXC3 diffractometer and irradiated with graphite-monochromated Cu-K_α radiation (λ = 1.54178 Å) for data collections. Lattice parameters were determined by least-square fitting of 31 reflections for all compounds with 31° < 2θ < 35° for **3l** and with 54° < 2θ < 60° for **2n** and **3n**. Data were collected with the 2θ/ω scan mode. All data were corrected for absorption[21] and extinction.[22] The structures were solved by a direct method and refined by full-matrix least-squares methods with the TeXsan program.[23] All non-hydrogen atoms were refined with anisotropic thermal parameters. All hydrogen atoms were included in the refinement on calculated positions (length of C–H: 1.0 Å) riding on their carrier atoms with isotropic thermal parameters.

CCDC-281932 (for **3l**), -154409 (for **2n**), and -154410 (for **3n**) contain the supplementary crystallographic data (CIF) for this paper. These data can be obtained free of charge from The Cambridge Crystallographic Data Centre via www.ccdc.cam.ac.uk/data_request/cif.

Kinetic Measurements of the Pseudorotation of 2k–n: Crude samples (ca. 5 mg) after work-up of the mixtures of **2k** and **3k** (1:1), **2l** and **3l** (1:1), and **2m** and **3m** (3:2) or a sample of **2n** (ca. 5 mg) dissolved in freshly distilled solvent (0.5–0.6 mL) were sealed separately in NMR tubes under N_2. ^{19}F NMR spectra were measured in variable temperature mode (error within ± 1 °C). The observed temperatures were calibrated with the ^{1}H NMR chemical shift difference of signals of neat 1,3-propanediol (high temperature region) and MeOH (low temperature region). The kinetic data were analyzed by assuming irreversible first-order kinetics using the equation $\ln(c_0/c) = kT$, in which c_0 = concentration of reactant at t = 0, c = concentration of reactant at arbitrary intervals. The activation enthalpies and entropies were calculated according to the transition state theory of Eyring by linear regression.

Acknowledgments

The authors are in debt to Dr. Shiro Matsukawa for providing technical assistance. The authors are grateful to Central Glass Co. Ltd. for a generous gift of hexafluorocumyl alcohol. Partial support of this work through Grants-in-Aid for Scientific Research (Nos. 06740488 and 07740501) provided by the Ministry of Education, Science, and Culture of the Japanese Government is heartily acknowledged.

[1] *Chemistry of Hypervalent Compounds* (Ed.: K-y. Akiba), Wiley-VCH, New York, **1999**.
[2] For *N-X-L* designation, see: C. W. Perkins, J. C. Martin, A. J. Arduengo, W. Lau, A. Alegria, J. K. Kochi, *J. Am. Chem. Soc.* **1980**, *102*, 7753–7759.
[3] a) G. C. Pimentel, *J. Chem. Phys.* **1951**, *19*, 446–448; b) R. J. Hach, R. E. Rundle, *J. Am. Chem. Soc.* **1951**, *73*, 4321–4324; c) J. I. Musher, *Angew. Chem. Int. Ed. Engl.* **1969**, *8*, 54–68.
[4] a) E. L. Muetteries, W. Mahler, R. Schmutzler, *Inorg. Chem.* **1963**, *2*, 613–618; b) R. R. Holmes, *Pentacoordinated Phosphorus−Structure and Spectroscopy*; ACS Monograph 175, 176; American Chemical Society, Washington, DC, **1980**, vol. I, II; c) J. C. Martin, *Science* **1983**, *221*, 509–514; d) D. E. C. Corbridge, *Phosphorus: Outline of Its Chemistry, Biochemistry, and Technology*, 4th ed., Elsevier, Amsterdam, **1990**, chapter 14, pp. 1233–1256; e) R. Burgada, R. Setton, *In The Chemistry of Organophosphorus Compounds* (Ed.: F. R. Hartley), Wiley-Interscience, Chichester, U.K., **1994**, vol. 3, pp. 185–272.
[5] R. S. Berry, *J. Chem. Phys.* **1960**, *32*, 933–938.
[6] a) R. M. Beesley, C. K. Ingold, J. F. Thorpe, *J. Chem. Soc.* **1915**, *107*, 1080; b) C. K. Ingold, *J. Chem. Soc.* **1921**, *119*, 305.
[7] a) S. Kojima, K. Kajiyama, M. Nakamoto, K.-y. Akiba, *J. Am. Chem. Soc.* **1996**, *118*, 12866–12867; b) S. Kojima, K. Kajiyama, M. Nakamoto, S. Matsukawa, K.-y. Akiba, *Eur. J. Org. Chem.* **2006**, 218–234.
[8] a) K. Kajiyama, M. Yoshimune, M. Nakamoto, S. Matsukawa, S. Kojima, Y. Yamamoto, K.-y. Akiba, *Org. Lett.* **2001**, *3*, 1873–1875; b) S. Matsukawa, S. Kojima, K. Kajiyama, M. Nakamoto, Y. Yamamoto, K.-y. Akiba, S.-Y. Re, S. Nagase, *J. Am. Chem. Soc.* **2002**, *124*, 13154–13170.
[9] K. Kajiyama, S. Kojima, K.-y. Akiba, *Tetrahedron Lett.* **1996**, *37*, 8409–8412.
[10] a) I. Granoth, J. C. Martin, *J. Am. Chem. Soc.* **1979**, *101*, 4618–4622 and 4623–4626; b) M. R. Ross, J. C. Martin, *J. Am. Chem. Soc.* **1981**, *103*, 1234–1235.
[11] a) S. Trippett, *Phosphorus Sulfur* **1976**, *1*, 89–98; b) S. Trippett, *Pure Appl. Chem.* **1970**, *40*, 595–605; c) G. Buono, J. R. Llinas, *J. Am. Chem. Soc.* **1981**, *103*, 4532–4540; d) R. R. Holmes, *J. Am. Chem. Soc.* **1978**, *100*, 433–446; e) S. Matsukawa, K. Kajiyama, S. Kojima, S.-y. Furuta, Y. Yamamoto, K.-y. Akiba, *Angew. Chem. Int. Ed.* **2002**, *41*, 4718–4722.
[12] G. M. Whitesides, M. Eisenhut, W. M. Bunting, *J. Am. Chem. Soc.* **1974**, *96*, 5398–5407.
[13] a) R. R. Holmes, J. A. Deiters, *J. Am. Chem. Soc.* **1977**, *99*, 3318–3326; b) R. R. Holmes, *Acc. Chem. Res.* **1979**, *12*, 257–265.
[14] E. L. Muetterties, L. J. Guggenberger, *J. Am. Chem. Soc.* **1974**, *96*, 1748–1756.
[15] a) R. Faw, C. D. Montgomery, S. J. Rettig, B. Shurmer, *Inorg. Chem.* **1998**, *37*, 4136–4138; b) K. Kajiyama, Y. Hirai, T. Otsuka, H. Yuge, T. K. Miyamoto, *Chem. Lett.* **2000**, *29*, 784–785.
[16] S. Kojima, Y. Doi, M. Okuda, K.-y. Akiba, *Organometallics* **1995**, *14*, 1928–1937.
[17] For leading references involving the turnstile mechanism see: a) I. Ugi, D. Marquarding, H. Klusacek, P. Gillespie, F. Ramirez, *Acc. Chem. Res.* **1971**, *4*, 288–296; b) P. Gillespie, P. Hoffman, H. Klusacek, D. Marquarding, S. Pfohl, F. Ramirez, E. A. Tsolis, I. Ugi, *Angew. Chem. Int. Ed. Engl.* **1971**, *10*, 687–715; c) F. Ramirez, I. Ugi, *Adv. Phys. Org. Chem.* **1971**, *9*, 25–126; d) R. R. Holmes, *Acc. Chem. Res.* **1972**, *5*, 296–303; e) P. Gillespie, F. Ramirez, I. Ugi, D. Marquarding, *Angew. Chem. Int. Ed. Engl.* **1973**, *12*, 91–119; f) S.-K. Shih, S. D. Peyerimhoff, R. J. Buenker, *J. Chem. Soc., Faraday Trans. 2* **1979**, *75*, 379–389; g) P. Lemmen, R. Baumgartner, I. Ugi, F. Ramirez, *Chem. Scripta* **1988**, *28*, 451–464.
[18] S. Kajigaeshi, M. Moriwaki, T. Tanaka, S. Fujisaki, *J. Chem. Soc., Perkin Trans. 1 Chem. Soc., Perkin Trans. 1* **1990**, 897–899.
[19] S. Kojima, K. Kajiyama, K.-y. Akiba, *Bull. Chem. Soc. Jpn.* **1995**, *68*, 1785–1797.
[20] S. Kajigaeshi, T. Kakinami, H. Tokiyama, T. Hirakawa, T. Okamoto, *Bull. Chem. Soc. Jpn.* **1987**, *60*, 2667–2668.
[21] A. Furusaki, *Acta Crystallogr., Sect. A* **1979**, *35*, 220.
[22] C. Katayama, *Acta Crystallogr., Sect. A* **1986**, *42*, 19.
[23] TeXsan: Single Crystal Analysis Software, version 1.9; Molecular Structure Corporation: The Woodlands, Texas 77381. USA, **1998**. The program was previously available from Mac Science Co.

Received: January 16, 2006
Published Online: April 3, 2006

